

Turbulent Friction in Rough Pipes and the Energy Spectrum of the Phenomenological Theory

G. Gioia and Pinaki Chakraborty

Department of Theoretical and Applied Mechanics
University of Illinois at Urbana-Champaign, Urbana, IL 61801

(Dated: November 26, 2024)

The classical experiments on turbulent friction in rough pipes were performed by J. Nikuradse in the 1930's. Seventy years later, they continue to defy theory. Here we model Nikuradse's experiments using the phenomenological theory of Kolmogórov, a theory that is widely thought to be applicable only to highly idealized flows. Our results include both the empirical scalings of Blasius and Strickler, and are otherwise in minute qualitative agreement with the experiments; they suggest that the phenomenological theory may be relevant to other flows of practical interest; and they unveil the existence of close ties between two milestones of experimental and theoretical turbulence.

Turbulence is the unrest that spontaneously takes over a streamline flow adjacent to a wall or obstacle when the flow is made sufficiently fast. Although most of the flows that surround us in everyday life and in nature are turbulent flows over rough walls, these flows have remained amongst the least understood phenomena of classical physics [1, 2]. Thus, one of the weightier experimental studies of turbulent flows on rough walls, and the most useful in common applications, is yet to be explained theoretically 70 years after its publication. In that study [3], Nikuradse elucidated how the friction coefficient between the wall of a pipe and the turbulent flow inside depends on the Reynolds number of the flow and the roughness of the wall. The friction coefficient, f , is a measure of the shear stress (or shear force per unit area) that the turbulent flow exerts on the wall of a pipe; it is customarily expressed in dimensionless form as $f = \tau/\rho V^2$, where ρ is the density of the liquid that flows in the pipe and V the mean velocity of the flow. The Reynolds number is defined as $Re = VR/\nu$, where R is the radius of the pipe and ν the kinematic viscosity of the liquid. Last, the roughness is defined as the ratio r/R between the size r of the roughness elements (sand grains in the case of Nikuradse's experiments) that line the wall of the pipe and the radius of the pipe.

Nikuradse presented his data in the form of six curves, the log-log plots of f versus Re for six values of the roughness [3]. These curves are shown in Fig. 1. At the onset of turbulence [4], at a Re of about 3,000, all six curves rise united in a single bundle. At a Re of about 3,500, the bundle bends downward to form a marked *hump* and then it plunges in accord with Blasius's empirical scaling [5], $f \sim Re^{-1/4}$, as one by one in order of decreasing roughness the curves start to careen away from the bundle. After leaving the bundle, which continues to plunge, each curve sets out to trace a *belly* [6] as it steers farther from the bundle with increasing Re , then flexes towards a terminal, constant value of f that is in keeping with Strickler's empirical scaling [7], $f \sim (r/R)^{1/3}$. For seventy years now, our understanding of these curves has been aided by little beyond a pictorial narrative of

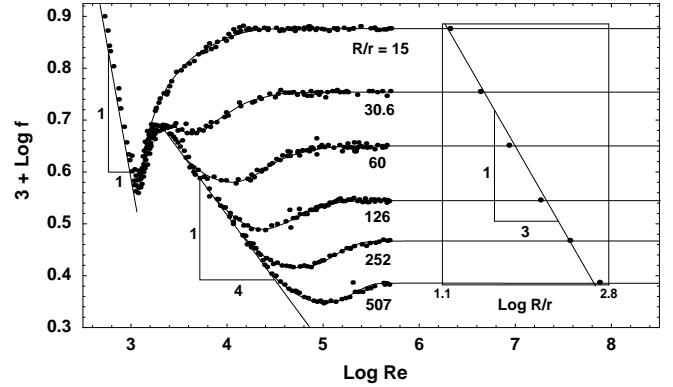


FIG. 1: Nikuradse's data. Up to a Re of about 3,000 the flow is streamline (free from turbulence) and $f \sim 1/Re$. Note that for very rough pipes (small R/r) the curves do not form a belly at intermediate values of Re . Inset: verification of Strickler's empirical scaling for f at high Re , $f \sim (r/R)^{1/3}$.

roughness elements being progressively exposed to the turbulent flow as Re increases [8].

In our theoretical work, we adopt the phenomenological imagery of "turbulent eddies" [9, 10, 11] and use the spectrum of turbulent energy [12] at a length-scale σ , $E(\sigma)$, to determine the velocity of the eddies of size s , u_s , in the form $u_s^2 = \int_0^s E(\sigma)\sigma^{-2}d\sigma$, where $E(\sigma) = A\varepsilon^{2/3}\sigma^{5/3}c_d(\eta/\sigma)c_e(\sigma/R)$. Here A is a dimensionless constant, ε is the turbulent power per unit mass, $\eta = \nu^{3/4}\varepsilon^{-1/4}$ is the viscous lengthscale, R is the largest lengthscale in the flow, $A\varepsilon^{2/3}\sigma^{5/3}$ is the Kolmogórov spectrum (which is valid in the inertial range, $\eta \ll \sigma \ll R$), and c_d and c_e are dimensionless corrections for the dissipative range and the energetic range, respectively. For c_d we adopt an exponential form, $c_d(\eta/\sigma) = \exp(-\beta\eta/\sigma)$ (which gives $c_d \approx 1$ except in the dissipative range, where $\sigma \approx \eta$), and for c_e the form proposed by von Kármán, $c_e(\sigma/R) = (1 + \gamma(\sigma/R)^2)^{-17/6}$ (which gives $c_e \approx 1$ except in the energetic range, where $\sigma \approx R$), where β and γ are dimensionless constants [12]. To obtain expressions for u_s and η in terms of Re , r/R , and

V , we invoke the usual scalings [13], $\varepsilon = \kappa_\varepsilon u_R^3/R$ (Taylor's scaling [14], where u_R is the characteristic velocity of the largest eddies and κ_ε a dimensionless constant) and $u_R = \kappa_u V$ (where κ_u is a dimensionless constant). Then, we can write $\eta = bR\text{Re}^{-3/4}$, where $b \equiv (\kappa_\varepsilon \kappa_u^3)^{-1/4}$, and (after changing the integration variable to $x \equiv \sigma/R$) $u_s^2 = A\kappa_\varepsilon^{2/3} u_R^2 \int_0^{s/R} x^{-1/3} c_d(b\text{Re}^{-3/4}/x) c_e(x) dx$. For $s \ll R$ we can set $c_e = 1$, compute the integral, and let $\text{Re} \rightarrow \infty$ to obtain $u_s^2 = (3/2)A\kappa_\varepsilon^{2/3} u_R^2 (s/R)^{2/3}$, or $u_s^2 \sim u_R^2 (s/R)^{2/3}$, a well-known result of the phenomenological theory. Further, for consistency with Taylor's scaling we must have $A\kappa_\varepsilon^{2/3} = 2/3$ (so that $u_s = u_R$ for $s = R$) and therefore $u_s^2 = \kappa_u^2 V^2 (2/3) \int_0^{s/R} x^{-1/3} c_d(b\text{Re}^{-3/4}/x) c_e(x) dx$.

We now seek to derive an expression for τ , the shear stress on the wall of the pipe. We assume a viscous layer of constant thickness $a\eta$, where a is a dimensionless constant, and call W a wetted surface parallel to the peaks of the viscous layer (Fig. 2). Then, τ is effected by momentum transfer across W . Above W , the velocity of the flow scales with V , and the fluid carries a high horizontal momentum per unit volume ($\sim \rho V$). Below W , the velocity of the flow is negligible, and the fluid carries a negligible horizontal momentum per unit volume. Now consider an eddy that straddles the wetted surface W . This eddy transfers fluid of high horizontal momentum downwards across W , and fluid of negligible horizontal momentum upwards across W . The net rate of transfer of momentum across W is set by the velocity normal to W , which velocity is provided by the eddy. Therefore, if v_n denotes the velocity normal to W provided by the *dominant* eddy that straddles W , then the shear stress effected by momentum transfer across W scales in the form $\tau \sim \rho V v_n$.

In order to identify the dominant eddy that straddles W , let us denote by $s = r + a\eta$ the size of the largest eddy that fits the coves between successive roughness elements. Eddies much larger than s can provide only a negligible velocity normal to W . (This observation is purely a matter of geometry.) On the other hand, eddies smaller than s can provide a sizable velocity normal to W . Nevertheless, if these eddies are much smaller than s , their velocities are overshadowed by the velocity of the eddy of size s . Thus, v_n scales with u_s , which is the velocity of the eddy of size s , and the dominant eddy is the largest eddy that fits the coves between successive roughness elements. We conclude that $\tau \sim \rho V u_s$, or $\tau = \kappa_\tau \rho V u_s$ (where κ_τ is a dimensionless constant of order 1), and therefore $f = \kappa_\tau u_s/V$ or

$$f = K \left(\int_0^{s/R} x^{-1/3} c_d(b\text{Re}^{-3/4}/x) c_e(x) dx \right)^{1/2}, \quad (1)$$

where $K \equiv \kappa_\tau \kappa_u \sqrt{2/3}$, $s/R = r/R + ab\text{Re}^{-3/4}$, and $b \equiv (\kappa_\varepsilon \kappa_u^3)^{-1/4}$. Equation (1) gives f as an explicit function

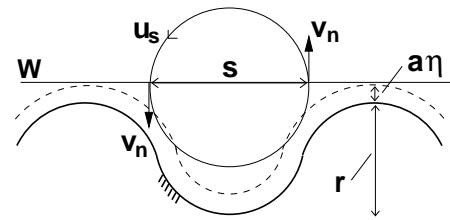


FIG. 2: Schematic of the immediate vicinity of the wall with roughness elements of size r covered by a viscous layer of uniform thickness $a\eta$. The distance between roughness elements is about equal to the height of the roughness elements, as in Nikuradse's experiments [20]. The horizontal line is the trace of a wetted surface W tangent to the peaks of the viscous layer.

of the Reynolds number Re and the roughness r/R .

To evaluate computationally the integral of (1), we set $\beta = 2.1$, $\gamma = 6.783$ (the values given in [12]), $a = 5$ (5η being a common estimation of the thickness of the viscous layer), $\kappa_\varepsilon = 5/4$ (a value that follows from Kolmogórov's four-fifth law [15]), $\kappa_u = 0.036$ (0.036 ± 0.005 being the value measured in pipe flow by Antonia and Pearson [16]), $b \equiv (\kappa_\varepsilon \kappa_u^3)^{-1/4} = 11.4$, and treat κ_τ as a free parameter (albeit a parameter constrained by theory to be of order 1). With $\kappa_\tau = 0.5$ (and therefore $K = 0.015$), (1) gives the plots of Fig. 3. (Note that a different value of κ_τ would give the same plots except for a vertical translation.) These plots show that (1) is in excellent qualitative agreement with Nikuradse's data, right from the onset of turbulence, including the hump and, for relatively low roughness, the bellies. These plots remain qualitatively the same even if the value of any of the parameters is changed widely. In particular, there is always a hump and there are always bellies: these are robust features closely connected with the overall form of the spectrum of turbulent energy. The connections will become apparent after the discussion that follows.

To help interpreting our results, we compute f without including the correction for the energetic range—that is, setting $\gamma = 0$. In this case, the integral of (1) may be evaluated analytically, with the result

$$f = K(r/R + ab\text{Re}^{-3/4})^{1/3} \sqrt{F(y)}, \quad (2)$$

where $F(y) = y^{2/3} \Gamma_{-2/3}(y)$, $\Gamma_{-2/3}$ is the gamma function of order $-2/3$, and $y = \beta\eta/s = \beta b\text{Re}^{-3/4}(r/R + ab\text{Re}^{-3/4})^{-1}$. With the same values of κ_τ , κ_u , a , b , and β as before, (2) gives the solid-line plots in the inset of Fig. 3. The hump is no more. We conclude that the hump relates to the energetic range. Further, with the exception of the hump at relatively low Re , the plots of (1) coincide with the plots of (2); thus, we can study (2) to reach conclusions about (1) at intermediate and high Re . For example, (2) gives $f \sim (r/R)^{1/3}$ for $r \gg a\eta$ and $f \sim \text{Re}^{-1/4}$ for $r \ll a\eta$. It follows that both (2) and (1) give a gradual transition between the empirical scalings

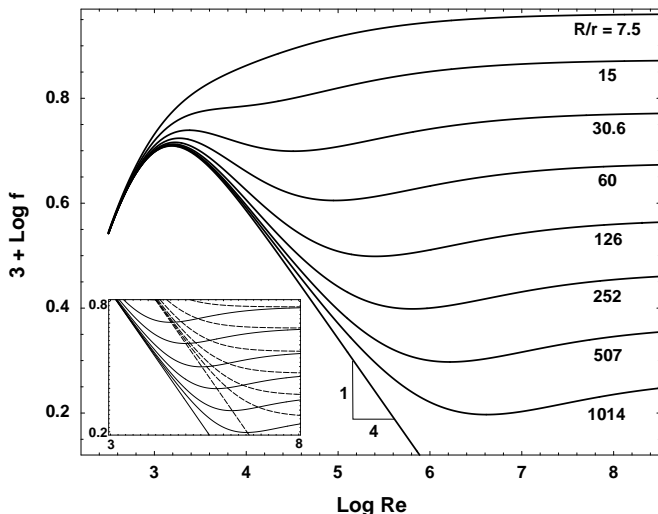


FIG. 3: Plot of (1). Inset: Plot of (2) (no correction for the energetic range: solid lines) and plot of (2) with $\gamma = 0$ (no correction for the energetic range and the dissipative range: dashed lines).

of Blasius and Strickler [17], in accord with Nikuradse’s data.

If we set $\beta = 0$ in addition to $\gamma = 0$, (2) simplifies to $f = \kappa_\tau \kappa_u (r/R + ab \text{Re}^{-3/4})^{1/3}$. With the same values of κ_τ , κ_u , a , and b as before, this expression gives the dashed-line plots in the inset of Fig. 3. Now the bellies are no more. We conclude that the bellies relate to the dissipative range. The dissipation depresses the values of f at relatively low and intermediate Re , leading to the formation of the bellies of Nikuradse’s data.

We are ready to explain the unfolding of Nikuradse’s data in terms of the varying habits of momentum transfer with increasing Re (Fig. 4). At relatively low Re , the inertial range is immature, and the momentum transfer is dominated by eddies in the energetic range, whose velocity scales with V , and therefore with Re . Consequently, an increase in Re leads to a more vigorous momentum transfer—and to an increase in f . This effect explains the rising part of the hump. At higher Re , the momentum transfer is dominated by eddies of size $s \approx a\eta \gg r$. Since $\eta \sim \text{Re}^{-3/4}$, with increasing Re the momentum transfer is effected by ever smaller (and slower) eddies, and f lessens as Re continues to increase. This effect explains the plunging part of the hump—the part governed by Blasius’s scaling. At intermediate Re , $s = r + a\eta$ with $r \approx a\eta$. Due to the decrease in η , s continues to lessen as Re continues to increase, but at a lower rate than before, when it was $s \approx a\eta \gg r$. Thus, the curve associated with r deviates from Blasius’s scaling and starts to trace a belly. As η continues to decrease, the dominant eddies become decidedly larger than the smaller eddies in the inertial range, which is well established now, and any lingering dissipation at lengthscales larger than s must

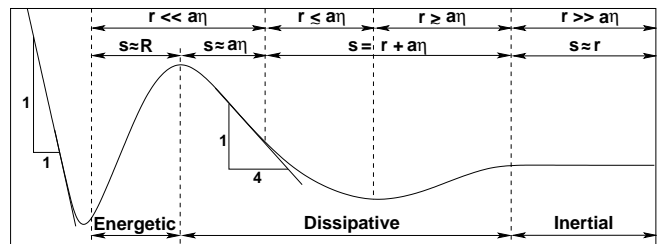


FIG. 4: Schematic of the relations among a generic Nikuradse curve, the spectrum of turbulent energy, the size of the roughness elements, the thickness of the viscous layer, and the size of the dominant eddies.

cease. This effect explains the rising part of the belly. Last, at high Re , $s \approx r \gg a\eta$. As Re increases further, η lessens and new, smaller eddies populate the flow and become jumbled with the preexisting eddies. Yet the momentum transfer continues to be dominated by eddies of size r , and f remains invariant. This effect explains Nikuradse’s data at high Re , where f is governed by Strickler’s scaling.

We have predicated equation (1), on the assumption that the turbulent eddies are governed by the phenomenological theory of turbulence. The theory was originally derived for isotropic and homogeneous flows, but recent research [18] suggests that it applies to much more general flows as well. Our results indicate that even where the flow is anisotropic and inhomogeneous—as is the case in the vicinity of a wall—the theory gives an approximate solution that embodies the essential structure of the complete solution (including the correct scalings of Blasius and Strickler) and is in detailed qualitative agreement with the observed phenomenology. Remarkably, the qualitative agreement holds starting at the very onset of turbulence, in accord with experimental evidence that “in pipes, turbulence sets in suddenly and fully, without intermediate states and without a clear stability boundary” [4]. The deficiencies in quantitative agreement point to a need for corrections to account for the effect of the roughness elements on the dissipative range as well as for the effect of the overall geometry on the energetic range.

In conclusion, to a good approximation the eddies in a pipe are governed by the spectrum of turbulent energy of the phenomenological theory. The size of the eddies that dominate the momentum transfer close to the wall is set by a combination of the size of the roughness elements and the viscous lengthscale. As a result, the dependence of the turbulent friction on the roughness and the Reynolds number is a direct manifestation of the distribution of turbulent energy given by the phenomenological theory. This close relation between the turbulent friction and the phenomenological theory [19] may be summarized in the following observation: the similarity exponents of Blasius and Strickler are but recast forms of the exponent $5/3$ of the Kolmogorov spectrum.

We are thankful to F. A. Bombardelli, N. Goldenfeld, and W. R. C. Phillips for a number of illuminating discussions. We are also thankful to Referee C, whose pointed criticism resulted in a much stronger paper. J. W. Phillips kindly read our manuscript and made suggestions for its improvement.

-
- [1] J. Jiménez, *Annu. Rev. Fluid Mech.* **36**, 173 (2004).
- [2] M. R. Raupach, R. A. Antonia, S. Rajagopalan, *Appl. Mech. Rev.* **44**, 1 (1991).
- [3] Reprinted in English in J. Nikuradse, *NACA TM 1292* (1950).
- [4] B. Hof et al., *Science* **305**, 1594 (2004).
- [5] L. Prandtl, *Essentials of Fluid Dynamics*, (Blackie & Son, London, 3rd ed., 1953), chap. III.11.
- [6] In Nikuradse’s experiments the average distance between roughness elements, λ , was about the same as the height of the roughness elements, r . This is the type of single-lengthscale roughness that concerns us here. For this type of roughness, there are always bellies in the log-log plots of f vs. Re . (For similar results on open channels, see Varwick’s data in, e.g., O. Kirshmer, *Revue générale de l’hydraulique* **51**, 115 (1949); in French.) For more complicated types of roughness, where roughness elements of many different sizes are present (as is commonly the case in commercial pipes), the bellies may be absent (see, e.g., the paper by Kirshmer cited above) or perhaps present after all (see, e.g., C. F. Colebrook, C. M. White, *Proc. Roy. Soc. London A* **161**, 367 (1937)). For the latest experimental data and discussion of this issue see J. J. Allen, M. A. Shockling, and A. J. Smits, *Evaluation of a universal transitional resistance diagram for pipes with honed surfaces* (to appear in *Phys. Fluids*) and M. A. Shockling, *Turbulent flow in a rough pipe*, MSE Dissertation (Princeton University, 2005).
- [7] Reprinted in English in A. Strickler, *Contribution to the question of a velocity formula and roughness data for streams, channels and close pipelines*, translation by T. Roesgen, W. R. Brownlie (Caltech, Pasadena, 1981). The value $1/3$ of the exponent of r/R in Strickler’s scaling can be derived by dimensional analysis from the value $2/3$ of the exponent of the hydraulic radius in Manning’s empirical formula for the average velocity of the flow in a rough open channel. Manning obtained his formula independently of Strickler, on the basis of different experimental data.
- [8] See, e.g., V. T. Chow, *Open-Channel Hydraulics* (McGraw-Hill, New York, 1988).
- [9] L. F. Richardson, *Proc. Roy. Soc. London A* **110**, 709 (1926).
- [10] Reprinted in English in A. N. Kolmogórov, *Proc. R. Soc. London A* **434**, 9 (1991).
- [11] U. Frisch, *Turbulence* (Cambridge Univ. Press, Cambridge, 1995).
- [12] S. B. Pope, *Turbulent Flows* (Cambridge Univ. Press, Cambridge, 2000).
- [13] See, e.g., H. Tennekes, J. L. Lumley, *A First Course in Turbulence* (MIT Press, 1972).
- [14] G. I. Taylor, *Proc. Roy. Soc. London A* **151**, 421 (1935); D. Lohse, *Phys. Rev. Lett.* **73**, 3223 (1994). The existence of an upper bound on ε that is independent of the viscosity has been proved *mathematically*; see Doering, Ch. R. and P. Constantin, *Phys. Rev. Lett.* **69**, 1648 (1992).
- [15] Kolmogorov’s four-fifth law reads $\overline{u_r^3} = -(4/5)\varepsilon r$, where the left-hand side is the third-order structure function. Substituting $r = R$ and estimating $|\overline{u_r^3}| = u_R^3$ leads to $\varepsilon = (5/4)u_R^3/R$, or $\kappa_\varepsilon = 5/4$. Experimental estimates of κ_ε are $O(1)$; see K. R. Sreenivasan, *Phys. Fluids* **10**, 528 (1998).
- [16] R. A. Antonia and B. R. Pearson, *Flow, Turbulence and Combustion* **64**, 95 (2000). For comparison, Tennekes and Lumley give $\kappa_u = 0.033$ for the atmosphere’s turbulent boundary layer [13].
- [17] G. Gioia, F. A. Bombardelli, *Phys. Rev. Lett.* **88**, 014501 (2002).
- [18] B. Knight, L. Sirovich, *Phys. Rev. Lett.* **65**, 1356 (1990); T. S. Lundgren, *Phys. Fluids* **14**, 638 (2002); T. S. Lundgren, *ibid.* **15**, 1024 (2003). Yet the view of anisotropy as a perturbation superposed on the isotropic flow (see, e.g., L. Biferale, I. Procaccia, *Anisotropy in turbulent flows and in turbulent transport*, arXiv:nlin.CD/0404014 (2004)) might break down close to a wall, where the exponents themselves might change (see M. Casciola, P. Gualtieri, B. Jacob, R. Piva, *Phys. Rev. Lett.* **95**, 024503 (2005)). Nevertheless, note (i) that the exponent of the second-order structure function appears to change only by little and (ii) that the Kolmogórov exponent does give the exact scalings of Blasius and Strickler, whereas any modified exponent would not.
- [19] The close connection between the turbulent friction and the phenomenological spectrum suggests that in turbulence, just as in phase transitions, large-scale phenomena are direct manifestations of the small-scale statistics. The parallel with phase transitions has been adduced by N. Goldenfeld, who was prompted by our results to reanalyze Nikuradse’s data and conclude that (2) is consistent with a turbulent analogue of Widom scaling near critical points. See N. Goldenfeld, *Roughness-induced critical phenomena in a turbulent flow*, arXiv:cond-mat/0509439 (2005).
- [20] Our schematic of Fig. 2 may seem to resemble the “d-type roughness” of A. E. Perry, W. H. Schofield, and P. N. Joubert, *J. Fluid Mech.* **37**, 383 (1969). According to these authors, for this type of roughness the turbulent friction does not asymptotically approach a constant value at high Re . Nevertheless, as pointed out by Jimenez [1], the distinction between k-type roughness (including the type of roughness in Nikuradse’s pipes) and d-type roughness appears to have been predicated on limited experimental data, and must be regarded with caution. In any case, the schematic of Fig. 2 represents the rough walls of Nikuradse’s experiments [6] and does lead to predictions that are in accord with those experiments.